

## THEORETICAL DESCRIPTION OF MOLECULE–METAL INTERACTION AND SURFACE REACTIONS

B.I. LUNDQVIST, O. GUNNARSSON \* and H. HJELMBERG

*Institute of Theoretical Physics, Chalmers University of Technology, S-412 96 Göteborg,  
Sweden*

and

J.K. NØKSKOV

*Institute of Physics, University of Aarhus, DK-8000 Aarhus C, Denmark*

Received 22 March 1979

Recent progress in the theoretical description of the interaction between molecules and metal surfaces and the reactivity of metal surfaces and of chemisorbed molecules is described. Electronic factors affecting associative and dissociative chemisorption, sticking, surface chemiluminescence and other surface reactions are illustrated with a few examples. In these dynamical processes several important features can be distinguished: the downward shift of molecular affinity levels upon approaching the surface and the fact that the active region usually lies outside the static equilibrium position studied by common spectroscopies. Further, the high reactivity of metals can in several cases be traced back to the fundamental and unique property of metals having a quasi-continuous spectrum of electronic excitations. The qualitative concepts and considerations are based on results of self-consistent calculations on simple models that stress the extended nature of the conduction-electron states. In a few cases the implications have been tested by dynamical experiments.

### 1. Introduction

In their interaction with molecules, metal surfaces often show a high reactivity. Their ability to break chemical bonds, to chemisorb and to recombine fragments, and their efficiency in energy transfer have been mentioned as factors affecting the chemical reactivity of metals. Wide variations in activity exist, however, and specificity is a rule rather than an exception. For instance, despite the general high ability of metals to dissociate molecules, several systems have been clearly identified, in which adsorption requires an appreciable activation energy.

\* Present address: IFF, KFA Jülich, D-5170 Jülich, German Fed. Rep.

The characteristic feature of metals is their quasicontinuous spectrum of electronic excitations, in particular the absence of a gap at the Fermi level. The purpose of this paper is to show that the high reactivity may be linked to this fundamental metallic property. This perspective is delineated on the background of a progress report of our recent work in this area.

The scene for this presentation could have been set by the Gstaad colloquium on the physical basis for heterogeneous catalysis in 1974 [1]. In its discussion of critical theory issues in this field, many relevant concepts were aired, such as electronically adiabatic potential-energy surfaces, nonadiabatic processes, molecular orbitals, local densities of states, and the Woodward–Hoffman rules for conservation of orbital symmetry. On the other hand, it was then too early for the colloquium to reach any firm conclusion on, e.g., the status of the adiabatic approximation. Neither were any explicit results on the expected connections between the concepts and the surface reactions available at that time.

The progress reported in this paper is based on model calculations and considerations and to some extent on experiments on elementary surface reactions. With the view that the identification of qualitative trends and concepts at present is much more productive than the aiming at quantitative agreement, we will review recent work on atomic and molecular chemisorption on free-electron like metals [2–6], on proposed electronic mechanisms for photon and electron emission in exothermic surface reactions [7,8], for the sticking of adsorbates [9] and for a surface reaction of the Eley–Rideal type, namely disproportionation of CO on Ni surfaces [10].

Features of the adsorbate-induced electron structure are central for the considerations. Therefore, section 2 is devoted to a review of results for it in self-consistent model calculations and to some generalizations thereof. Results for potential-energy curves are given and discussed in section 3. In section 4, the importance of non-adiabatic electronic transitions for the reactivity is discussed. Some explicit surface reactions are described in section 5. The concluding remarks in section 6, finally, dwell upon some general aspects on the considerations of this paper.

## 2. Adsorbate-induced electron structure

A certain understanding of the changes in the electronic structure caused by the interaction of an atom or molecule with a metal surface is a prerequisite for the discussion of electronic mechanisms in surface processes. With the aim to demonstrate general trends and qualitative features we will in this section review self-consistent results for the adsorbate-induced electron structure from model calculations [2–6,11], attempt to formulate general rules for it, and compare with the results of other types of self-consistent chemisorption calculations.

Our calculations utilize the Kohn–Sham scheme [12], which provides a good description of the interaction between the electrons [13,14]. The Kohn–Sham

equations can be written as

$$\left( -\frac{\hbar^2 \nabla^2}{2m} + V_{\text{eff}}(\mathbf{r}) \right) \varphi_i(\mathbf{r}) = \epsilon_i \varphi_i(\mathbf{r}), \quad (1)$$

where  $V_{\text{eff}}(\mathbf{r})$  is the effective one-electron potential felt by the electrons at the point  $\mathbf{r}$  and  $\varphi_i(\mathbf{r})$  are orbital amplitudes, giving the electronic density as

$$n(\mathbf{r}) = \sum_i^{\text{occ}} |\varphi_i(\mathbf{r})|^2. \quad (2)$$

Although the energy parameters  $\epsilon_i$  have no formal relation to the one-electron excitation spectrum, the levels and densities of states (DOS)

$$n(\epsilon) = \sum_i \delta(\epsilon - \epsilon_i) \quad (3)$$

derived from them have, indeed, bearings on the ground-state properties [12,13] and are frequently close to the one-electron excitation spectrum [14,15]. We will also describe the electron structure in terms of the local density of states (LDOS)

$$n(\mathbf{r}, \epsilon) = \sum_i |\varphi_i(\mathbf{r})|^2 \delta(\epsilon - \epsilon_i), \quad (4)$$

the density

$$n(\mathbf{r}) = \int_{-\infty}^{\epsilon_F} d\epsilon n(\mathbf{r}, \epsilon), \quad (5)$$

where  $\epsilon_F$  is the Fermi level, and the projected densities of states

$$n_a(\epsilon) = \sum_i |\langle a | \varphi_i \rangle|^2 \delta(\epsilon - \epsilon_i), \quad (6)$$

where  $|a\rangle$  is some appropriate state.

To describe the metal substrate the jellium model [16] has been used. It treats the metal ions by smearing them out to a homogeneous (bulk) or semi-infinite (surface) constant background of positive charge. One advantage of it is that it is fully characterized by one quantity, the constant bulk electron density  $n_0 = (4\pi r_s^3/3)^{-1}$  au, often described by the parameter  $r_s$ . By varying this fundamental parameter, trends and characteristic behaviours in different physical ranges can be found. The use of the jellium model for explorative surface studies [14,16] has an instructive parallel in bulk solid state physics. There the Sommerfeld model of metals has had an enormous success in giving a qualitative explanation of metallic properties. Just as in the case of the perfect three-dimensional crystal [17], a hierarchy of improved models can later be introduced for the surface, to account for lattice effects, d electrons etc.

*H in jellium (Je).* A proton placed in an infinite jellium, i.e. in a homogeneous

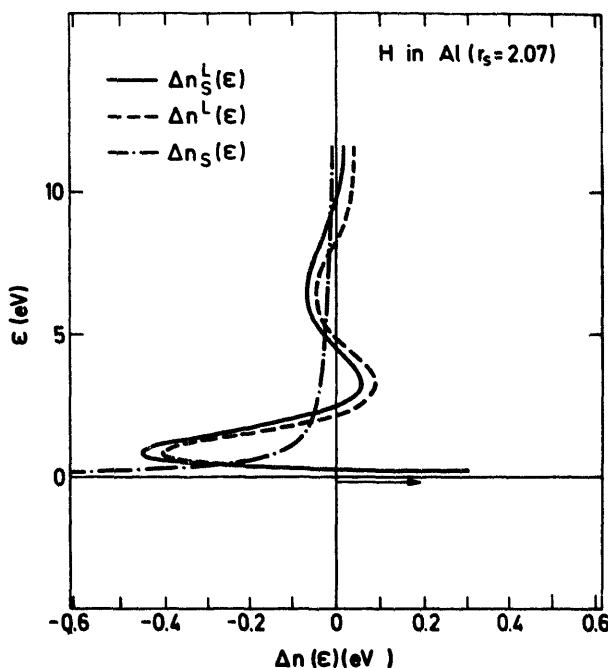


Fig. 1. The impurity-induced density of states (DOS) for hydrogen in jellium at  $r_s = 2.07$ , corresponding to Al [19]. The local induced DOS  $\Delta n^L$  describes states within a radius of 10 au around the proton. Also shown are the s-components of this quantity,  $\Delta n_s^L$ , and of the total DOS,  $\Delta n_s$ .

electron liquid, is only a limiting case in this context. As we shall see, it is a useful one. For  $r_s$  values larger than 1.9, the hydrogen-induced DOS shows a shallow bound state (fig. 1), which is doubly occupied in the ground state [18,19]. Through the whole metallic-density region, this split-off,  $H^-$ -like state has an energy very close to the bottom of the conduction band and is extremely delocalized. A hydrogen impurity in jellium can therefore be regarded as a heavily screened  $H^-$  ion ( $H^-/Je^+$ ). It appears that a self-consistent, spin-polarized calculation with the bound state only singly occupied ( $H/Je$ ) gives a split-off energy level also rather close to the bottom of the band [19,20]. This relatively small level shift between  $H/Je$  and  $H^-/Je^+$  should be contrasted with the corresponding, considerably larger one between free  $H$  and  $H^-$ . The latter shift is due to the Coulomb repulsion between the two electrons. Thanks to the existence of a bound state, the ground-state solution ( $H^-/Je^+$ ) works as an excellent illustration of the important role of the metallic conduction electrons in this context. In fig. 2 the bound-state density is compared with the screening density and the total H-induced density. It shows how the extra electron connected with the shallow bound state is screened out primarily by the conduction electrons in the bottom of the band (cf. fig. 1). Due to the long wavelength of the latter, the screening cloud is very extended, and the extremely delocalized bound electrons are screened out almost completely. Only a localized,  $H$ -like (rather than  $H^-$ -like) density and the Friedel oscillations survive in the total

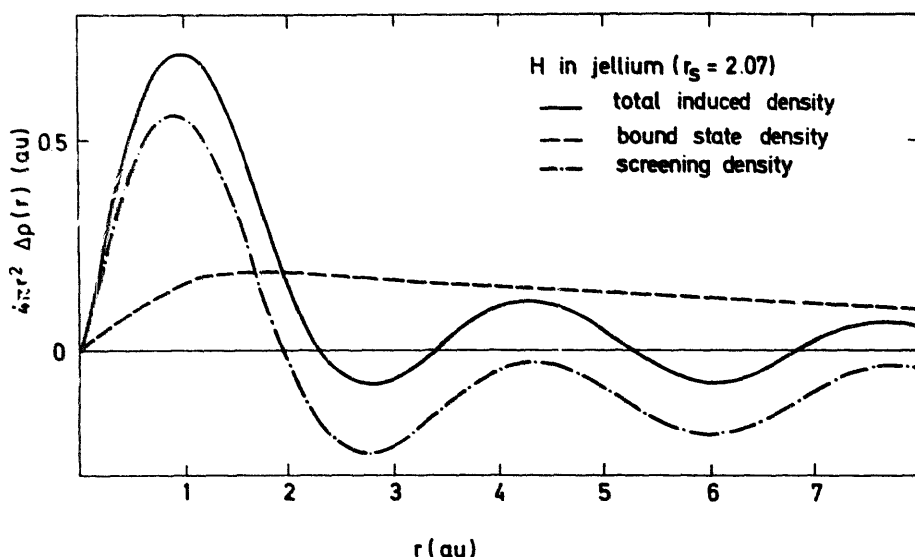


Fig. 2. The induced density  $4\pi r^2 \Delta\rho(r)$  for a hydrogen atom in jellium at  $r_s = 2.07$ , corresponding to Al, decomposed into bound state and screening charge contributions [19].

density. Thus the screening makes the proton-induced perturbations on the density and thus the potentials very localized. Just as important in this context is the fact that the extremely efficient screening properties of the conduction electrons helps to reduce the Coulomb repulsion between two bound electrons substantially. Fig. 2 shows that this is done by the bound state and screening charge densities interpenetrating each other. Thus the Coulomb shift of the bound level due to the double occupancy is small at typical metallic densities. The metallic screening, i.e. the high polarizability, is due to the absence of an energy gap at the Fermi level. Therefore one can state in a more general way that, *due to the quasi-continuous spectrum of the electronic excitations of metals, affinity levels are much more likely to be filled for atoms in a metallic environment than in the free atom.*

**H on Je.** The simplest conceivable chemisorption system should be a hydrogen atom at a jellium surface. When an H atom is approaching the surface, the interference with the substrate states should broaden [21] and shift the atomic levels [22]. The H/Je system is expected to be a weak-coupling system, i.e., one with atomic resonances or split-off states rather than one with separated bonding and antibonding levels [22]. The self-consistent calculations [2–4] confirm this picture, as illustrated by the DOS curves in fig. 3. Both the width and the position of the resonance vary with the distance  $d$  from the surface.

An extensive variation of the model parameters ( $r_s$  and  $d$ ) have clearly demonstrated that substrate properties significantly affect the energy of the atomic resonance. A correlation between the resonance and the effective electron potential  $V_{\text{eff}}^0$  of the clean jellium surface, earlier noticed for other adatoms on a single jellium surface [23], is clearly born out, when  $r_s$  is allowed to vary, as in fig. 4.

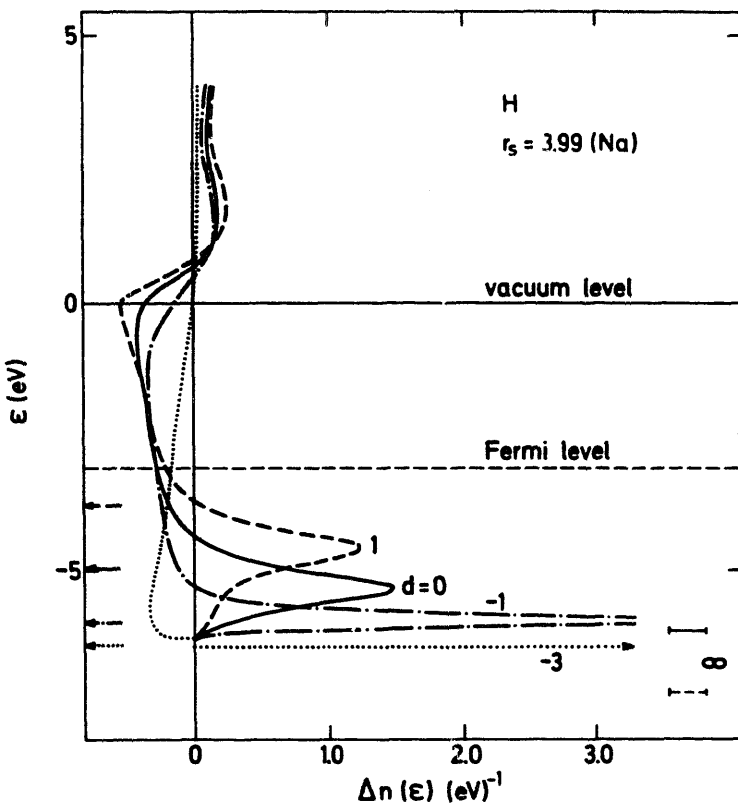


Fig. 3. The adatom-induced density of states  $\Delta n(\epsilon)$  for a hydrogen atom at a distance  $d$ (au) outside the edge of a semi-infinite jellium with  $r_s = 2.65$ , corresponding to Mg. The values of the clean-surface effective electron potential  $V_{\text{eff}}^0(d)$  is marked with an arrow to the left. To the right, the free-atom results are given both for a spin-polarized (dashed line) and an unpolarized calculation [4].

Close to the surface, therefore, the H-induced smeared-out level is expected to be shifted downwards as rapidly as  $V_{\text{eff}}^0(d)$ , when  $d$  decreases.

The H-induced resonance can be given several useful interpretations. One is the molecular orbital (MO) picture of Gurney [21]. It views states  $\varphi_i(r)$  with energies in the resonance region as jellium states that are enhanced around the proton. In a projected DOS like eq. (6), with  $|a\rangle$  taken as, e.g., a hydrogen 1s state, this shows up as a resonance. The width of the latter is given by

$$\Delta_a = \pi \sum_k |V_{ak}|^2 \delta(\epsilon_a - \epsilon_k) \quad (7)$$

in the Newns-Anderson model [22]. Here  $\epsilon_a$  is the atomic resonance energy,  $\epsilon_k$  the energy of the substrate state  $|k\rangle$ , and  $V_{ak}$  the coupling between  $|a\rangle$  and  $|k\rangle$ . This width is a measure of the decay rate of the adatom state  $|a\rangle$  [21]. The decay occurs as a hopping of the electron into substrate states  $|k\rangle$  [24].

Another question concerns whether the H-induced resonance is H- or H<sup>-</sup>-like. As

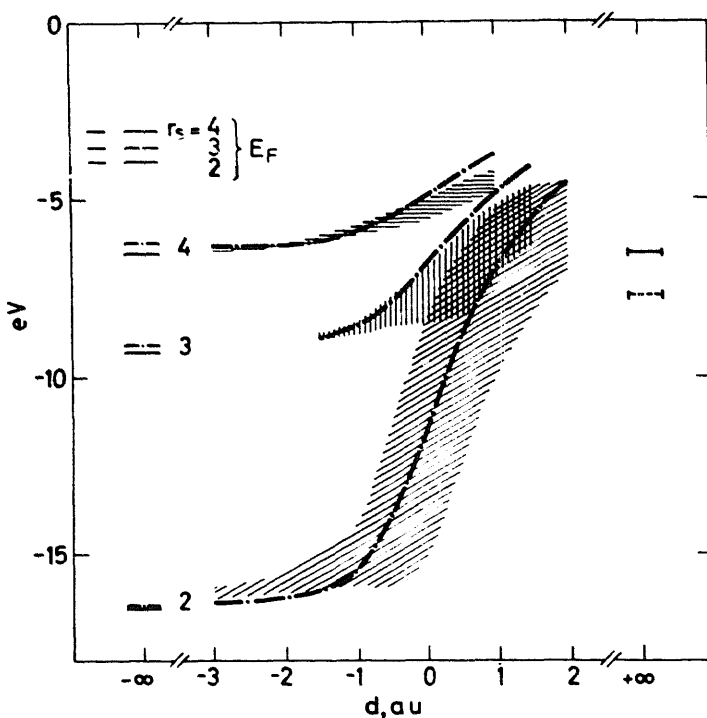


Fig. 4. The peak position (shaded area) in the H-induced density of states [4], as a function of the distance  $d$  between the H atom and the jellium edge, is shown for the different  $r_s$  values. The dash-dotted curves give the effective electron potential of the clean surface,  $V_{\text{eff}}^0(d)$ . To the left ( $d = -\infty$ ), the bulk results [18] are given. To the right ( $d = \infty$ ), the free-atom results are given both for a spin-polarized (dashed line) and an unpolarized (full line) calculation.

described in the previous paragraph, it is neither. It is a resonance, and a unique separation into orbital and screening charge cannot be made. Still, it is useful to know how a certain atomic level develops upon approaching the surface. The state correlation diagram of fig. 5, for the  $(N+1)$ -electron system of H and jellium, where  $N$  is the number of electrons of the clean jellium, is most helpful for this purpose. It is based on values for the total energies, calculated within the Kohn–Sham scheme using the local-density approximation [19,25]. For the separated species,  $\text{H} + \text{Je}$  is the ground state, and  $\text{H}^- + \text{Je}^+$  is obtained by transferring one electron from the Fermi level of the jellium to the affinity level of H. The latter state lies an amount  $\phi - A$  higher in energy, where  $\phi$  is the clean jellium work function [16] and  $A$  the electron affinity of H [25]. In the unified limit, double occupancy of the bound state ( $\text{H}^-/\text{Je}^+$ ) gives a considerably lower total energy than single occupancy ( $\text{H}/\text{Je}$ ) [19]. The line correlating  $\text{H}^- + \text{Je}^+$  and  $\text{H}^-/\text{Je}^+$  crosses the line between  $\text{H} + \text{Je}$  and  $\text{H}/\text{Je}$  and the numerous lines (not shown in the figure) that correspond to excited holes in the conduction band. This should occur in the surface region. In an electronically adiabatic potential-curve diagram, most of these crossings should be avoided ones, due to the low symmetry of the problem. In fig. 5 only the ground-state potential curve is schematically drawn as a smooth curve

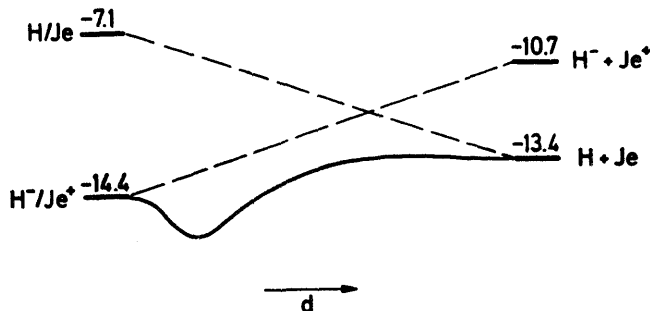


Fig. 5. Schematic state correlation diagram for unified ( $H/Je$  and  $H^-/Je^+$ ) and separated ( $H^- + Je^+$  and  $H + Je$ ) hydrogen and jellium. The energy values (in eV) are taken from ref. [19].

from  $H + Je$  to  $H^-/Je^+$ , corresponding to the adiabatic potential-energy curve discussed in the next section.

On the other hand, the  $H^-/Je^+$  state correlates with  $H^- + Je^+$ . The system cannot go between these limits in an adiabatic way, however. For atoms in relative motion (at energies ranging from about 0.1 eV to about 1 keV) a class of quasi-stationary electronic states, called diabatic states, have appeared to give a more appropriate description of the mutual interactions [26]. Frequently, such a diabatic state corresponds to a simple physical configuration of the electrons. The broken lines of fig. 5 are such diabatic levels. The nature of the diabatic state, whose level is indicated schematically by a dashed line in fig. 6 is that of an affinity state. As both end points have bound  $H^-$ -like states, it is natural to conceptually regard also the resonances in the surface region as doubly occupied, broadened  $H^-$  levels plus a screening charge, connected with the deformation of the conduction electron distribution. In the ground-state calculations this interpretation applies for  $d$  smaller than at least 2 au according to fig. 4, where a major part of the resonance lies below the Fermi level [3].

Out of the results and discussions above, there emerges the following picture: *As an atom approaches a metal surface, its affinity level is shifted downwards, in a way that is strongly influenced by the effective electron potential of the clean surface,  $V_{\text{eff}}^0$ .* The prevailing picture in the literature [27] thereby becomes a little more systematic and quantified.

*$H_2$  in  $Je$ .* The pseudo-molecular interaction of  $H_2$  embedded in jellium has been studied by a one-center extension of the method for  $H$  in  $Je$  [19]. It appears that the MO concept is still useful, however in a generalized sense. The interaction between the impurities can be described in terms of bonding and antibonding MO-like states/resonances. The bonding-antibonding splittings are reduced by screening effects (fig. 7), the bonding MO having a sharp level below the bottom of the conduction band. For  $H_2$  the most significant difference between a free and an embedded molecule is that the antibonding MO resonance of the latter is broadened, shifted in energy and partially filled (fig. 8). The filling, which in turn controls the pseudo-

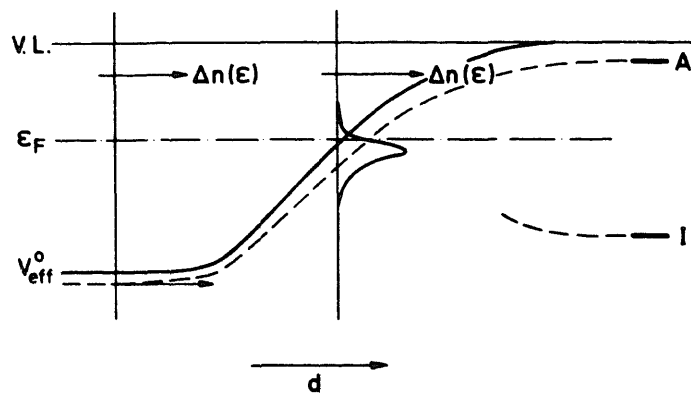


Fig. 6. Schematic drawing of the hydrogen-induced one-electron spectrum for the H-Je system in its ground state, for varying distances  $d$  between the proton and the jellium edge. The vacuum level (V.L.), the work function  $\phi$ , the Fermi level ( $\epsilon_F$ ) and the bottom of the conduction band ( $V_{\text{eff}}^0$ ) of the substrate are marked, as well as the affinity ( $A$ ) and ionization levels ( $I$ ) of the free H atom. The dashed curve indicates the variation of the level for the non-adiabatic state, leading to the  $H^-$  ion upon rapid separation.

molecular binding energy, is found to increase with increasing electron density of the surrounding jellium (fig. 8). This is a consequence of the antibonding MO resonance having an energy slightly above the bottom of the band and a width not varying too much with  $r_s$ . The picture of a molecule gradually drowning and decomposing, as the surrounding conduction-electron density increases, develops in this way.

*H<sub>2</sub> on Je.* So far self-consistent model calculations have been performed only for

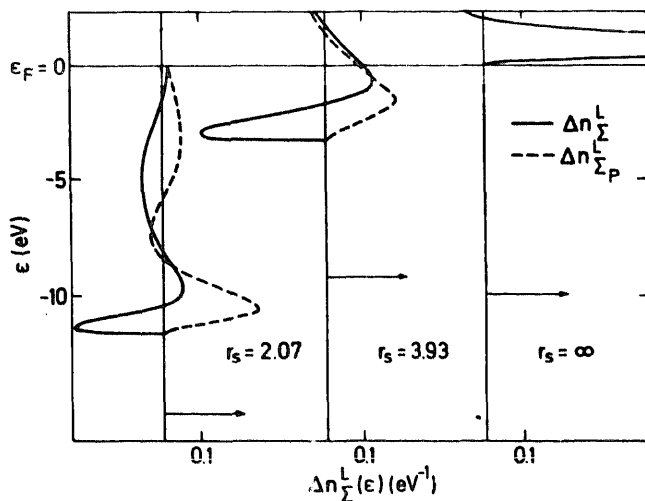


Fig. 7. The local induced density of states for free  $H_2$  and  $H_2$  in jellium for  $r_s = 2.07$  and  $3.93$ , corresponding to Al and Na, respectively. Only the parts with  $\Sigma$  and  $\Sigma_p$  (relating to the  $2\sigma^*$  MO) symmetry are given.

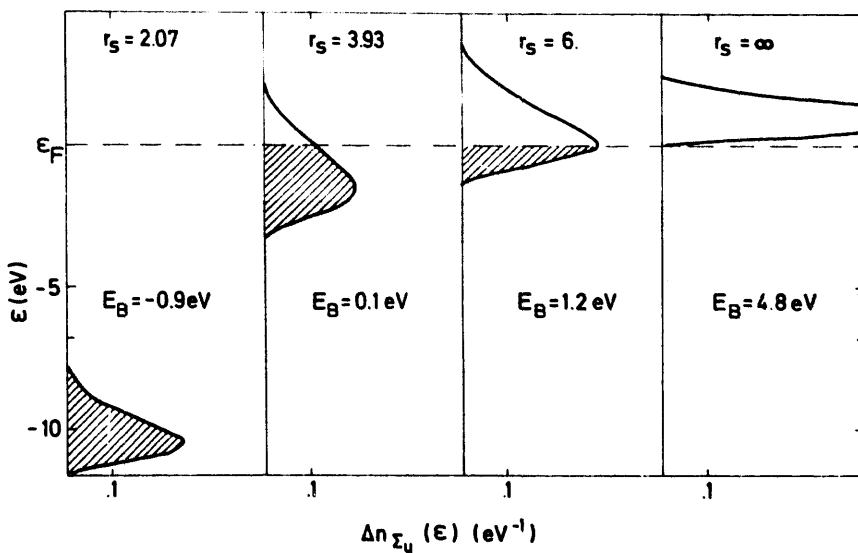


Fig. 8. The  $\Sigma_u$  (odd with respect to inversions about the molecular center and cylindrically symmetrical around the axis) projection of the induced density of states for  $H_2$  in jellium at different densities,  $r_s = 2.07$  corresponding to Al, 3.93 to Na and  $\infty$  to vacuum. The  $\Sigma_u$  projection picks out the states that are antibonding with respect to the H-H bond. The antibonding resonance is seen to get filled as  $r_s$  decreases (density increases). Subsequently, the binding energy  $E_B$  decreases [5].

$H_2$  standing upright on the jellium surface [6]. The essential features of an extrapolation [5] of the bulk results [19] are confirmed (fig. 9). The bonding MO level is split-off below the bottom of the band. Upon approaching the metal surface, the molecule gets its antibonding  $2\sigma^*$  affinity level shifted downwards, thus allowing a successive filling of the antibonding resonance. The downshift has a certain correlation with the effective electron potential of the clean surface  $V_{\text{eff}}^0(d)$ . It does not follow  $V_{\text{eff}}^0(d)$  as closely as does the H-induced resonance in the H-on-Je-case, which has a dominant s-character. It appears that the symmetry and localization of the MO's modify the correlation [6]. An adatom state with a certain symmetry primarily interferes with substrate states with the same symmetry in the adatom region. Therefore, the bottom of the local, symmetry-projected density of states of the clean surface should be a good point of aim for the location of an adatom resonance with a given symmetry [11]. For an adatom with s-symmetry this coincides with the bottom of the local density of states (summed over all symmetries), i.e., with  $V_{\text{eff}}^0(d)$ .

The charge and orbital-charge contours of fig. 10 show, how the chemisorption bond is building up between the inner proton and the jellium and how the filling of the  $\tilde{\sigma}^*$  MO resonance gives electronic charge on the outer H atom. To understand this better and to see the reduced bonding-antibonding separation, due to the screening, we compare in fig. 11 the  $H_2$ -induced DOS with those induced by the H atoms in the same position but without any intramolecular interaction [6]. From

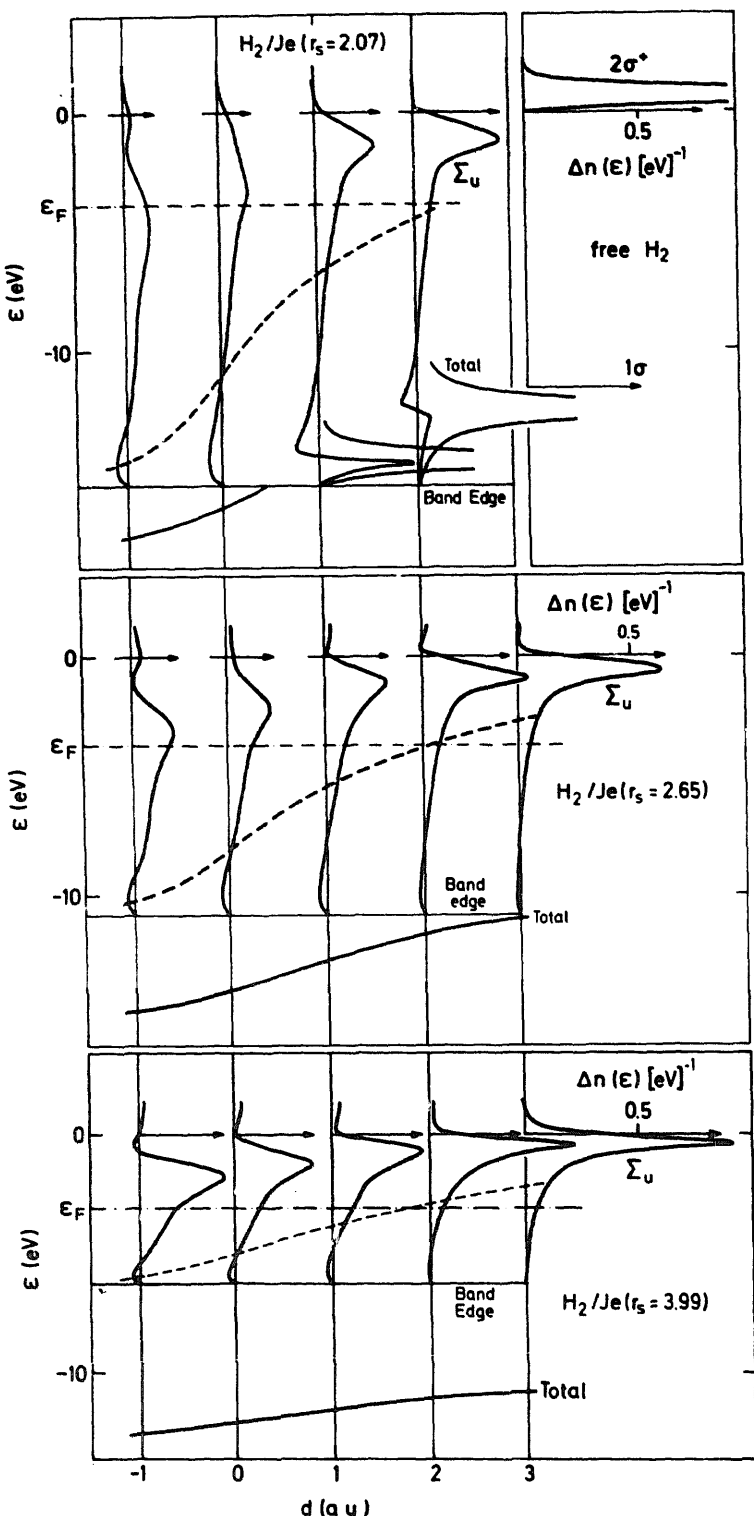


Fig. 9.  $H_2$ -induced density of states (DOS),  $\Delta n(\epsilon)$ , for  $H_2$  standing upright on a jellium surface, as a function of the distance  $d$ , between the surface and the midpoint of  $H_2$ , with  $r_s = 2.07$  (Al), 2.65 (Mg) and 3.99 (Na). The  $\tilde{\Sigma}_u$  MO resonance is identified with the  $\Sigma_u$  projection of  $\Delta n(\epsilon)$  (the  $\tilde{1}\sigma$  MO, denoted “total” in the figure, contains all symmetries). The internuclear distance is  $R = 1.4$  au. The dashed curve denotes  $V_{\text{eff}}^0(d)$ , the effective electron potential of the clean jellium surface. In the upper right corner the free  $H_2$  DOS is drawn as a comparison [6].

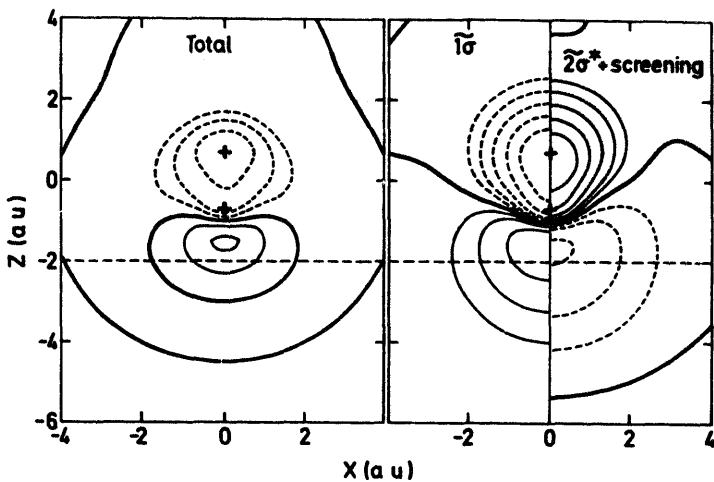


Fig. 10. Orbital charge density contours for  $H_2$  perpendicular to and at  $d = 2$  au outside a jellium surface with  $r_s = 2.65$  (Mg). The  $\tilde{1}\sigma$  density corresponds to the bound state density minus the density of a free  $H_2$  molecule. The “ $\tilde{2}\sigma^*$  + screening” density corresponds to all the states in the band below the Fermi energy, i.e.

$$\int_{V_{\text{eff}}^0(-\infty)}^{\epsilon_F} d\epsilon \Delta n(r, \epsilon).$$

The contours to the left are the sum of these two densities. The internuclear distance is  $R = 1.4$  au [6].

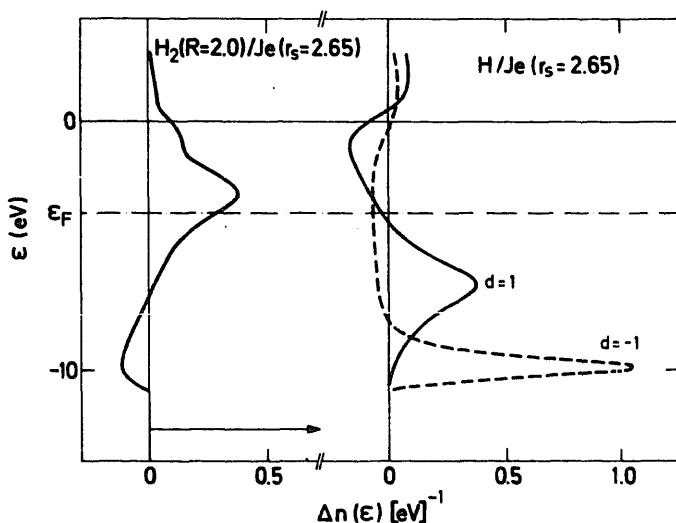


Fig. 11. Induced DOS  $\Delta n(\epsilon)$  for two widely separated H atoms at  $d = -1$  and 1 au, compared to that for a  $H_2$  molecule with an internuclear distance  $R = 2.0$  au at  $d = 0$  au outside a jellium surface ( $r_s = 2.65$ , Mg) [6].

in this picture it is obvious that in the given geometry the bonding  $\tilde{1}\sigma$  MO has more charge on the inner atom, i.e., on the atom having the lower atomic resonances, when isolated, and that the reverse is true for the upper, antibonding  $\tilde{2}\sigma^*$  MO resonance.

*Rule about affinity levels.* The results of the H and H<sub>2</sub> calculations in and on helium can be condensed into a simple principle: *The interaction with metals shifts affinity energy levels downwards and increases the population of them.* The latter can occur very efficiently on metals, as the Coulomb repulsion between two adsorbate electrons is reduced considerably, due to the screening by the conduction electrons. The mechanism has been clearly illustrated by the case of H<sup>-</sup> in Je<sup>+</sup>. It is intimately tied to the fundamental property of metals having a quasi-continuous electron excitation spectrum. Therefore the simple principle is likely to have a general applicability.

*Other model calculations.* There exist other self-consistent chemisorption calculations with other models and methods. A brief scan through the literature gives further support for the principle.

At the Gstaad meeting (ref. [1], p. 329), Grimley reported results for H on a simple model for Li that show the affinity level right down near the H 1s level in the free atom. This was interpreted as an effect of electrostatic (Madelung) stabilization.

The calculations by Lang and Williams for atomic H, O, Cl and Si on Je with  $r_s = 2.0$  [23] have been the first ones to draw the attention to the possible correlation between the adatom resonance position and the effective electron potential of the clean surface. The DOS curves for O and Cl in the equilibrium position on Je imply that the p-shells of adsorbed O and Cl get completely populated upon chemisorption.

The principle can to a certain extent also get illustrations from cluster calculations. In looking for electronic indices of surface reactivity, Johnson [28] has summarized investigations of the electronic structure of cluster and coordination complexes, utilizing the self-consistent field Xα scattered-wave density-functional approach to MO theory, in terms of a “spin-orbit electronegative” concept. Molecular-orbital calculations reviewed in ref. [28] and elsewhere [29] give examples of adsorbate affinity energy levels shifted downwards and filled due to the interaction with s-, p- and d-orbitals of transition-metal clusters. Discrete variational Xα calculations on carbonyl complexes and clusters as well as other calculations on clusters containing CO [30] illustrate, how the principle applies for the  $2\pi^*$  MO of CO through the so called  $\pi$  back-donation. As stressed in ref. [24] the adsorbate level shift is smaller on the less polarizable cluster than on an extended metal substrate, as illustrated for O/Al in refs. [23] and [29].

Supporting results can soon also be gathered from layer calculations. In a recent self-consistent pseudopotential calculation, using the local-density description of exchange and correlation effects, with a mixed basis and a super-cell description of the surface geometry, Louie [31] has shown an ordered (1 × 1) monolayer of

atomic hydrogen on the Pd(111) surface to give dramatic changes of the Pd electron structure. An occupied H–Pd bonding surface band centered at –6.5 eV below the Fermi level illustrates that also d electrons are efficient to fulfil the rule.

More illustrations can be found in recent reviews on the adsorbate-induced electron structure [24]. In particular, the downshift and filling of antibonding MO's have been earlier found in a systematic study of diatomic molecules interacting with clusters, using the Extended Hückel method [32].

### 3. Potential-energy curves

Molecular interaction with surfaces can occur through physisorption, i.e., through rather weak polarization forces, and chemisorption, i.e., through the intermingling of adsorbate and substrate electrons. The chemisorption may be associative or dissociative, where the chemisorbed species is split into fragments. For considerations about the thermodynamics of, e.g., such a dissociative adsorption, about the activation energy of the rate constant of a reaction or about the reaction path, the electronically adiabatic potential–energy surfaces are of key interest. In this context, the simple model for dissociative adsorption that was introduced by Lennard-Jones in 1933 [33] still plays a central role. Our recent self-consistent calculations for H<sub>2</sub> adsorption [6] support the Lennard-Jones description of molecular adsorption, however with a molecular potential–energy curve that is due to chemisorption rather than physisorption. They also give a certain insight into the nature of the chemisorption bond, shedding light on factors affecting atomic and molecular adsorption and the relation between these processes.

*H on Je.* Like the chemical bond of molecules [34] and the cohesive bond of solids [35], the adsorbate–substrate interaction is ultimately a result of a gain in potential energy, which is not completely balanced by the simultaneous increase in kinetic energy. Fig. 12 shows how, at the equilibrium distance, the electronic charge of adsorbed H is contracted compared with the free atom [2]. This contraction is the prime source of the binding, as it gives an increase in nuclear attraction (from –27 to –31 eV at  $r_s = 2$ ). The associated increase in kinetic energy in the region close to the nucleus is partially balanced by a reduction in the more distant region on the jellium side, due to the smoothing of the wavefunctions for low-lying bonding-type levels (fig. 13). The latter delocalization is ultimately caused by the sharing of the electrons. The balance between kinetic-energy increases and reductions is a delicate one, sensitive to the electron density (and thus  $r_s$ ) of the surrounding medium. As a simple uncertainty-relation argument would indicate, the cost in kinetic energy is higher the higher the density (the smaller  $r_s$ ).

These arguments give an immediate understanding of the calculated potential-energy curves in fig. 14. The strong  $r_s$ -dependence of the curves at small  $d$ -values are due to the increasing cost in kinetic energy with decreasing  $r_s$ . This strong variation with  $r_s$  makes the curves of fig. 14 illustrate three typical cases: one segregator ( $r_s =$

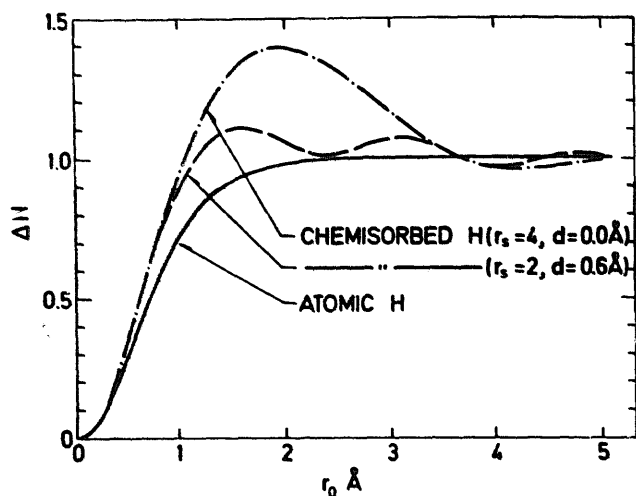


Fig. 12. The adatom-induced electron density  $\Delta\rho(r)$  for H in the equilibrium position outside a jellium surface, compared with the density of atomic hydrogen, plotted as the amount of electronic charge within a sphere of radius  $r_0$  [2]:

$$\Delta N(r_0) = \int_0^{r_0} r^2 dr d\Omega \Delta\rho(r).$$

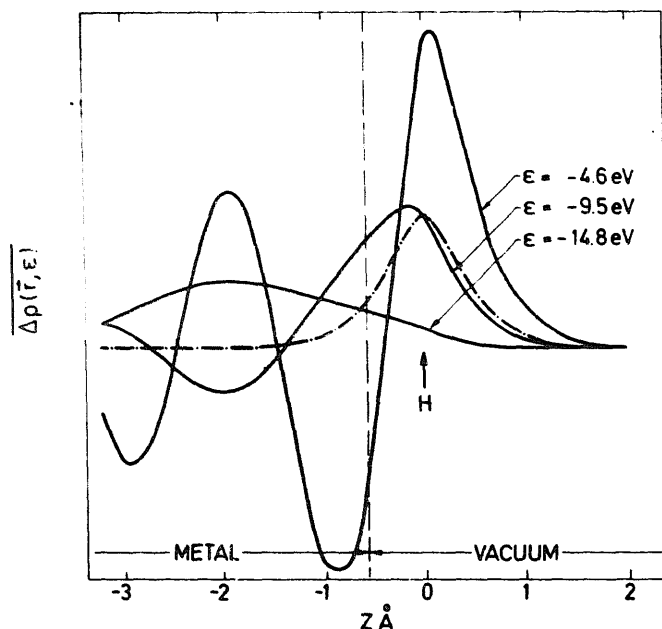


Fig. 13. Local density of states  $\Delta\rho(r, \epsilon)$  for hydrogen in equilibrium position ( $d = 0.6 \text{ \AA}$ ) on a jellium surface ( $r_s = 2$ ), plotted as the cylindrical average  $\Delta\rho(r, \epsilon) = \int r dr \int \phi d\phi \Delta\rho(r, \epsilon)$ , where cylindrical coordinates are chosen with  $z$  normal to the surface. The Kohn-Sham energy parameters  $\epsilon$  ( $\epsilon = 0$  corresponds to the vacuum level) range from close to the bottom of the band ( $\epsilon = -16.4 \text{ eV}$ ) to close to the Fermi level ( $\epsilon = -3.9 \text{ eV}$ ). The H resonance is about 4.1 eV wide and located around  $\epsilon = -7.0 \text{ eV}$ . The dashed curve gives  $\Delta\rho(r, \epsilon)$  for a free H atom in the same position. (The vertical scale is linear and the same for all curves.) The curves are normalized according to  $\int \Delta\rho(r, \epsilon) dz = 1$  [2].

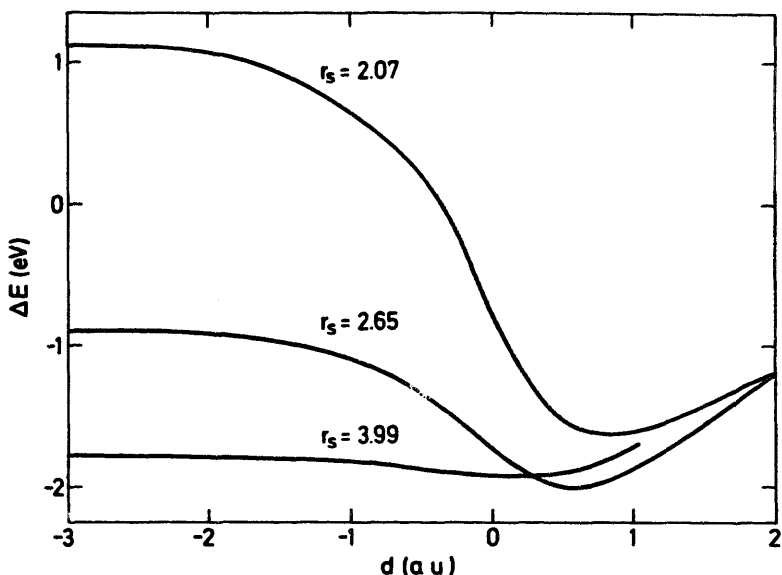


Fig. 14. The energy change upon chemisorption  $\Delta E(d)$  for H a distance  $d$  outside jellium at  $r_s = 2.07$  (Al), 2.65 (Mg) and 3.99 (Na) [4].

2.09), one absorber ( $r_s = 3.99$ ) and one intermediate case ( $r_s = 2.65$ ) [4].

By introducing corrections due to the discrete ion lattice, as in fig. 15 [6], more realistic energy considerations can be made. The potential–energy curve for H in a center position on a Mg(0001) surface has been calculated by lowest-order pertur-

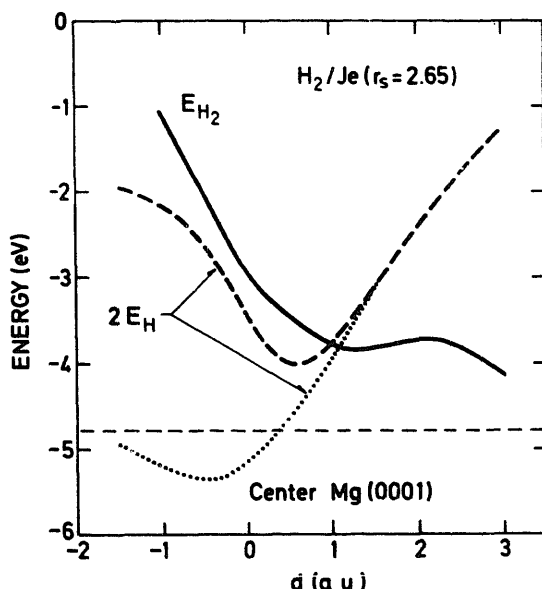


Fig. 15. The potential energy curve ( $E_{H_2}$ ) for  $H_2$  outside and normal to a jellium surface ( $r_s = 2.65$ , Mg) as a function of the distance  $d$  (full curve). The diagram also shows the potential–energy curves ( $2E_H$ ) of two H atoms infinitely apart with equal  $d$ , without (dashed curve) [4] and including lattice corrections corresponding to the center position of the Mg(0001) surface (dotted line) [2]. The internuclear distance of  $H_2$  is  $R = 1.4$  au [6].

bation theory with an array of pseudopotentials representing the lattice [2,4,23]. Thereby values for the binding energy and the vibrational frequencies and predictions about preferred adsorption sites can be extracted [2,4].

*H<sub>2</sub> on Je.* Upon approaching the surface, the H<sub>2</sub> molecule gets its 2σ\* level broadened and shifted downwards. *The resulting gradual filling of this antibonding MO resonance reduces the strength of the intra-molecular bond.* In a homogeneous electron liquid, this makes the interaction energy E<sub>B</sub> between two embedded H atoms one order of magnitude smaller than the free-molecule binding energy E<sub>B</sub> at low metallic densities, and at high metallic densities the interaction gets even repulsive [19].

This breaking of the molecular bond occurs simultaneously and in a certain competition with the building up of the chemisorption bond. Conceptually, it is useful to express the molecular chemisorption energy in terms of two contributions, the above-mentioned intra-molecular contribution and an extra-molecular one, due to the interaction of the individual H atoms with the metal substrate. That is

$$E_{H_2}(\mathbf{R}_1, \mathbf{R}_2) = E_{\text{intra}}(\mathbf{R}_1, \mathbf{R}_2) + E_{\text{extra}}(\mathbf{R}_1, \mathbf{R}_2), \quad (8)$$

where  $\mathbf{R}_1$  and  $\mathbf{R}_2$  are the positions of the two H atoms and

$$E_{\text{extra}}(\mathbf{R}_1, \mathbf{R}_2) = E_H(\mathbf{R}_1) + E_H(\mathbf{R}_2), \quad (9)$$

with  $E_H(\mathbf{R})$  denoting the chemisorption energy of a single H atom at a position  $\mathbf{R}$ .

Basically, both  $E_{\text{extra}}$  and  $E_{\text{intra}}$  result from the overlap between adsorbate and substrate electron states and the interference, which follows from this. The overlap effects enter in different ways, however, as can be seen from the above discussions of the nature of the chemisorption bond and of the shifting and filling of affinity resonances. Already in the simple jellium model this difference is apparent. As the two effects, due to their different origins, depend on  $r_s$  in different ways, several kinds of potential–energy curves can be generated by varying  $r_s$  [6]. The curves in fig. 16, calculated for H<sub>2</sub> standing upright on jellium, can be viewed as illustrating the three cases of a desorber ( $r_s = 2.07$ , Al), a dissociative adsorber ( $r_s = 2.65$ , Mg, see fig. 15) and an associative adsorber ( $r_s = 3.99$ , Na) [36]. The similar trends in the jellium curves for H (fig. 14) and H<sub>2</sub> (fig. 16) should be noticed. The rather deep valley of the potential–energy curve for  $r_s = 3.99$  goes over to a weak dent for  $r_s = 2.07$ . Once again the reason for this and the steeper shape of the repulsive wall at small distances  $d$  for the higher densities (smaller  $r_s$ ) is the increased kinetic energy, imposed by the reduced volume available for the adsorbate electrons.

At the larger  $d$ -values (greater than about 1 au), fig. 16 shows striking differences between the atomic ( $E_H$ ) and molecular curves ( $E_{H_2}$ ). While the former are rather  $r_s$ -independent, the  $E_{H_2}$  curves vary strongly with  $r_s$ . This is due to the  $E_{\text{intra}}$  term of eq. (8). As a matter of fact, this term can be rather well approximated by the interaction energy  $E_B$  of two H atoms at the same separation in a homogeneous electron liquid with a density equal to the one of the clean jellium surface at the molecular position [6]. As mentioned above,  $E_{\text{intra}}$  is a monotonically

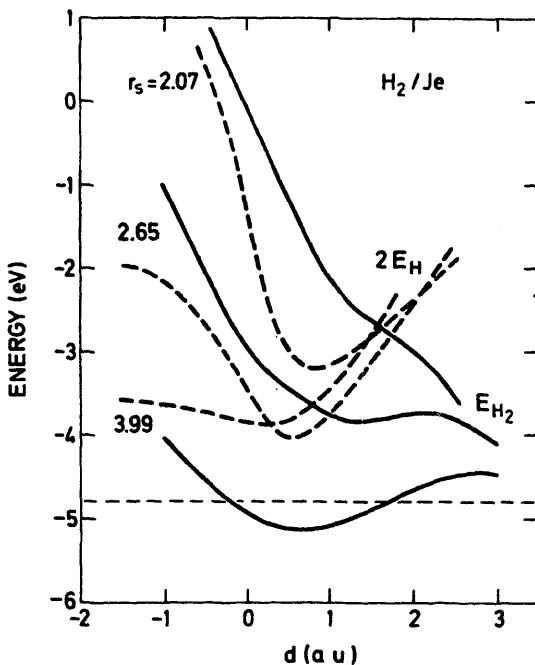


Fig. 16. Potential-energy curves ( $E_{H_2}$ ) for  $H_2$  normal to and outside jellium surfaces with  $r_s = 2.07$  (Al), 2.65 (Mg) and 3.99 (Na), as a function of the distance  $d$  (full curve). As a comparison the dashed curves give the potential-energy curves ( $2E_H$ ) of two H atoms infinitely apart with equal  $d$  [4]. The horizontal, dashed line gives  $E_{H_2}$  at  $d = \infty$ , i.e. the free  $H_2$  result. The inter-nuclear distance of  $H_2$  is taken as  $R = 1.4$  au [6].

cally increasing function of the density through the metallic density regime, due to the increasing filling of the antibonding resonance [19]. This means that (1) upon approaching the surface,  $E_{\text{intra}}$  is a growing function and (2) the growth starts further out from the surface and is stronger, the higher the bulk density (lower  $r_s$ ) is. These features are clearly reflected in the potential-energy curves of fig. 16.

In this manner, the questions about associative or dissociative adsorption, and about activated or non-activated dissociation find their answers in the relative sizes of  $E_{\text{extra}}$  and  $E_{\text{intra}}$  and in their relative variation as functions of the distance from the surface.

The mechanisms behind those effects have a fundamental nature. The above general considerations about the chemisorption bond apply to  $E_{\text{extra}}$ . The down-shift and the filling of the antibonding affinity resonance affect  $E_{\text{intra}}$ . Therefore, the concepts  $E_{\text{extra}}$  and  $E_{\text{intra}}$  and eq. (8) should be useful for molecular chemisorption systems in general. Such extension have to be made with care. In the general case the chemisorption bond and the filling of affinity resonances are not merely functions of  $r_s$ . Substrate factors, such as the discreteness of the ion lattice and, e.g., d electrons in transition metals, and adsorbate factors, such as the existence of several relevant molecular orbitals, can all affect the intra- and extra-molecular energies, not to mention geometrical effects. As these factors vary from one

surface to another and from one adsorbate to another, a rich variety of potential-energy curves can be obtained. This is the basis of the specificity of surface reactions.

In summary, *the downshift and filling of antibonding affinity resonances of molecules on metal surfaces plays an important role for the high reactivity of metals*. Thereby  $E_{\text{intra}}$  can become orders of magnitude less attractive than in the free molecule or repulsive. This makes the energy cost for new atomic configurations small.

*CO on transition metals.* As an illustration of how the considerations about the extra- and intra-molecular energies can be extended [6], we will give a tentative explanation of the observed trends about CO adsorption within the transition metal sequences. Carbon monoxide is known to adsorb molecularly on the fourth row transition metals to the right of Fe and on Fe at low temperatures and dissociatively on transition metals to the left of Fe and on Fe at high temperatures [37]. Similar trends apply for the transition metals of the fifth and sixth rows of the periodic system. The explanation has to contain thermodynamic considerations, such as comparing the chemisorption energies for associatively and dissociatively adsorbed CO, as well as considerations about kinetics, in particular describing the activation barrier on Fe.

The attention is focused on the  $2\pi^*$  orbital of CO. The increased population of this antibonding orbital on a transition-metal surface, mentioned in section 2, implies an increase in  $E_{\text{intra}}$  [30]. The latter quantity might even get positive, which is required for dissociation at zero temperature. The filling of  $\tilde{2}\pi^*$  levels also implies a strengthened chemisorption bond [38]. The donation of charge from the  $5\sigma$  MO, located around the C atom, is generally believed to give the most important contribution to the chemisorption bond. This MO interferes primarily with the s-electrons of the substrate and is thereby likely to determine the chemisorption bond length.

Now the  $2\pi^*$  MO interacts primarily with the d-states that can provide a proper symmetry. The overlap and thus the interference are stronger the more extended the d-electron states are. When going to the left in the transition-metal sequence, the d wavefunctions get more extended, due to the reduction in the effective atomic potential. This increased  $2\pi^*-d$  interference implies a consequential growth in  $E_{\text{intra}}$ , when going from Cu to Ti. The intramolecular energy  $E_{\text{intra}}$  might very well change from attractive to repulsive within the sequence, for instance for Fe.

In parallel, the extra-molecular energy  $E_{\text{extra}}$  gets more attractive, the further to the left in the sequence the substrate is placed. This should apply both for the molecular potential–energy curves, due to increased  $2\pi^*-d$  interference, and the atomic ones, due to increased p–d interference.

The above trends might be summarized in a Lennard-Jones potential–energy diagram where, upon moving from the right to the left in the transition-metal sequence, the atomic curve is lowered in energy in relation to the molecular curve. According to this picture, the disposition of CO to dissociate should be greater to the left in the transition-metal sequence than to the right, in agreement with experi-

mental findings. Here we have just indicated the consequence of one, albeit central, aspect, namely the qualitative effects of the interference between the  $2\pi^*$  MO and the d-electrons. To get more quantitative statements, other aspects, such as effects of geometry and of other molecular orbitals, should be considered. Also then, the conceptual model described here might be a useful alternative to cumbersome direct calculations of potential–energy curves.

*H<sub>2</sub> on Mg, Cu and Ni.* Fig. 15 [6], read literally, would imply that H<sub>2</sub> should be adsorbed dissociatively on the Mg(0001) surface. It also implies that dissociative adsorption should occur with an activation barrier, about 1 eV high. As mentioned earlier, the model and calculational accuracy is not aimed at that very quantitative statements. The results of fig. 15 nevertheless provide a useful starting point for qualitative and semi-quantitative considerations, such as the following one about the effects of various other factors on the activation barrier.

In the center position on Mg(0001), the lattice correction for H has a limited range [4b]. This should be true also for H<sub>2</sub> [6]. Fig. 15 indicates that its contribution to the activation barrier can be ignored for H<sub>2</sub> standing upright in the center position of Mg(0001). For H<sub>2</sub> atop of an Mg atom, on the other hand, it could give a distinguishable reduction, however not much more than about 0.1 eV [4]. For an H<sub>2</sub> molecule coming in parallel to the surface, the activation energy would probably be reduced even further, as the molecule then benefits from a more attractive extra-molecular energy (eq. (9)), caused by allowing the hydrogen atoms at R<sub>1</sub> and R<sub>2</sub> to be closer to the minimum of the E<sub>H</sub>(R) curve. Finally, the activation energy is expected to be reduced even further, by allowing the H–H distance to expand compared to the free-molecule bond length used in fig. 15. In summary, there are theoretical arguments for an activation energy of H<sub>2</sub> dissociation on Mg(0001) of about 1 eV or less.

Copper has an sp-electron average density close to that of Mg ( $r_s = 2.65$ ). In addition, it has a valence d-electron shell, which is filled. The barrier region lies outside the region of the d-electrons. Therefore, an approximation, where the effects of the d-electrons on the activation energy, are treated in a perturbative way, as a correction to the appropriate jellium results, should be reasonable.

The d-electrons give an extra coupling  $V_{d\sigma}$  to the  $2\sigma$  MO of H<sub>2</sub> [39]. A rough estimate for this interaction can be obtained from the Extended Hückel method [40]:

$$V_{d\sigma^*} \approx 0.875(\epsilon_d + \epsilon_{\sigma^*}) S_{d\sigma^*}, \quad (10)$$

where  $S_{d\sigma^*}$  is the overlap between the d<sub>yz</sub> and  $2\sigma^*$  orbitals and  $\epsilon_d$  and  $\epsilon_{\sigma^*}$  are the d and  $2\sigma$  orbital energies. The  $2\sigma^*$  level is shifted down to about the Fermi level by the interference with the sp-electrons. The extra binding is then roughly given by  $\Delta E \sim 2|V_{d\sigma^*}|^2/|\epsilon_{\sigma^*} - \epsilon_d|$ , as only the bonding-shifted level is expected to be occupied. We choose geometrical parameters as for H<sub>2</sub> lying parallel to the surface in the activation barrier region above an Mg atom, i.e. (at distances 1.7 and 2.2 Å), outside the first substrate layer for open and close-packed surfaces, respectively, and  $\epsilon_d \approx$

–6.5 eV and  $\epsilon_{\sigma^*} \approx -4.5$  eV. One can then estimate  $\Delta E$  to be roughly 0.04 and 0.3 eV on close-packed and open Cu surfaces, respectively [41]. This is not enough to remove the activation energy completely. For Ni, on the other hand, where the relevant d-level lies close to the Fermi level (and thereby close to  $\epsilon_{\sigma^*}$ ), the corresponding estimates (with  $\epsilon_d \approx \epsilon_{\sigma^*} \approx -4.5$  eV) for  $\Delta E \approx 2|V_{d\sigma}|$  are 0.3 and 0.9 eV for close-packed and open surfaces, respectively. Considering the fact that the effective conduction-electron density is slightly lower ( $r_s$  around 3, giving  $E_a \approx 0.6$  eV for H<sub>2</sub> perpendicular to the jellium surface) and the additional corrections discussed above, an activation barrier should be unlikely on all Ni surfaces and certainly absent on the open surfaces. In this way, the fact that the d-band lies higher up in energy in Ni than in Cu might be the explanation of the observed differences in activation energy between Cu ( $E_{act} = 0.25$  eV) and Ni ( $E_{act} < 0$ ) [42]. The incomplete filling of the d bands in Ni might give rise to a further reduction of the potential energy in the barrier region, due to static as well as dynamical spin polarizations.

**CO + CO on Ni.** The surface reactions discussed so far have been adsorption of H<sub>2</sub> and CO. The changes in the electronic structure of atoms and molecules on metal surfaces including the filling of molecular affinity levels, should be important for more general surface reactions, as well. To illustrate this, we will here briefly review a recent proposition about a mechanism for the catalytic action of Ni surfaces on the reaction



and its experimental confirmation [10]. The mechanism is based on qualitative considerations about changes in potential–energy surfaces caused by electronic redistributions occurring for molecules close to metal surfaces. The role of the surface is to circumvent energy and symmetry restrictions that exist for the corresponding gas-phase reaction. For the reaction (11) it appears that the chemisorption of the produced carbon is important for the thermodynamics, and that the partial filling of the  $2\pi^*$ -correlated levels of adsorbed CO is important for the reaction rate [10].

The proposition is based on vibrational electron energy loss (EEL) spectroscopy and low energy electron diffraction (LEED) observations regarding CO adsorption on the Ni(100), Ni(100)p(2 × 2)O, and Ni(100)c(2 × 2)O surfaces. The EEL spectra show that the C–O stretching vibrational frequencies are lower for adsorbed CO than for the free molecule, and that CO adsorbed on clean Ni(100) (at 295 K) has higher frequencies than CO adsorbed on the Ni(100)p(2 × 2)O surface (at 175 K). On the Ni(100)c(2 × 2)O surface on the other hand, CO adsorbs only at defects (at 175 K). In accordance with the correlation between reduction in stretching frequency and the population of the antibonding  $2\pi^*$  orbital, established for carbonyls [43], the back-donation model for CO adsorption on Ni [44] gets one of its more direct supports. The initially unoccupied  $2\pi^*$  MO of CO gets partially populated on Ni(100) and still more filled on Ni(100)p(2 × 2)O. There is thus a radical difference

in orbital occupancy between free and adsorbed CO and a quantitative difference in  $2\pi$  occupancy between the two surfaces.

A chemical reaction can be viewed as a deformation of a system of atoms from one configuration to another. The reactivity is related to the electronic response to such deformation, and the reaction path corresponds to deformations, for which the response is particular soft. A hint about the important charge transfer mechanisms can be obtained from the second-order expression for the total energy. The contribution that corresponds to a softening is [45]

$$\delta E = \sum_{n \neq 0} \frac{|\langle \phi_n | \delta V | \phi_0 \rangle|^2}{E_0 - E_n}, \quad (12)$$

where  $\delta V$  is the change in potential associated with a small deformation, and where  $\phi_n$  and  $E_n$  are the wavefunction and energy, respectively, of the total system,  $n = 0$  corresponding to the ground state. In eq. (12), low-lying excitations are essential for a soft response, provided that  $\phi_n$  and  $\phi_0$  have the same symmetry [45,46]. The EEL spectra imply that the highest occupied adsorbate induced orbitals, which have weight on CO, have a  $\pi$ -like symmetry. For a co-linear reaction



this matches the symmetry of the lowest unoccupied  $2\pi^*$  free CO orbital. Therefore, *chemisorption of one of the reactants provides low-lying electron–hole pair excitations of the right symmetry for a co-linear reaction, which are absent in the corresponding gas-phase reaction. This gives a lower activation barrier on the surface.*

The  $2\pi^*$ -like chemisorption level should actually be described as a group of resonance levels [21,22,30], i.e., a superposition of states having approximately the same energy and hence contributing almost equally to eq. (12). Therefore, the population of the resonance must be a key quantity, closely related to the catalytic activity. The higher population on Ni(100)p( $2 \times 2$ )O, revealed by the EEL measurements, thus should lead to a lower activation energy here than on clean Ni(100).

The mechanism has been confirmed through mass-spectroscopical registration of CO<sub>2</sub> formation during CO adsorption on the Ni(100)p( $2 \times 2$ )O and c( $2 \times 2$ )O surfaces [10]. In short, fig. 17 shows (i) that one of the reactants is adsorbed, as the observed CO<sub>2</sub> formation is significantly higher on p( $2 \times 2$ )O than on c( $2 \times 2$ )O, where there are no adsorbed CO molecules, and as the peak in the reaction rate on p( $2 \times 2$ )O around 300 K correlates with the surface coverage of CO, (ii) that one of the reactants is in the gas phase, as the rate on p( $2 \times 2$ )O depends linearly on the CO pressure, and (iii) that the activation energy is lower on the p( $2 \times 2$ )O pre-covered surface than on the clean Ni(100), as the reaction proceeds with a high rate above 250 and 450 K, respectively. Thus, the reaction proceeds according to eq. (13), i.e. it is of the Eley–Rideal type [47], and in the electronic mechanism for it filling of  $2\pi^*$  affinity levels of adsorbed CO is essential.

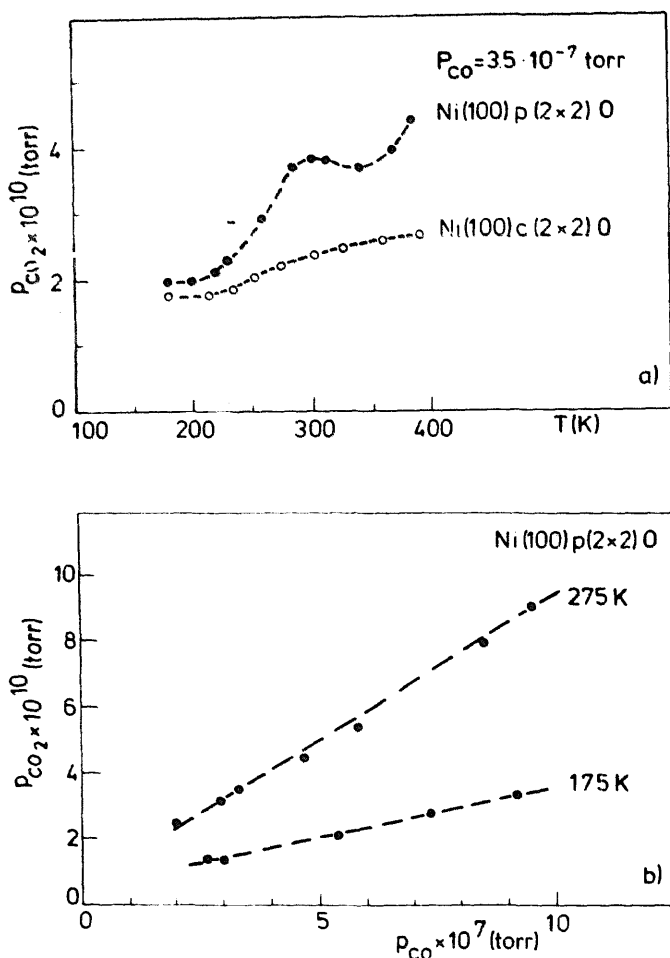


Fig. 17. Formation of CO<sub>2</sub> as a function of (a) specimen temperature, with CO pressure kept constant at  $3.5 \times 10^{-7}$  Torr, on Ni(100)p(2 × 2)C, Ni(100)c(2 × 2)O (in this temperature range same as for Ni(100)) and (b) CO pressure on p(2 × 2)O at two different specimen temperatures, 175 and 275 K [10].

#### 4. Non-adiabatic processes

The potential-energy curves, calculated within the adiabatic approximation, correspond to conservative forces on the molecule. If only they were around, only elastic processes would occur on the surface. A molecule approaching the surface would then initially be accelerated, then decelerated, then reflected and finally scattered off the surface, without loss of energy. This molecule–metal interaction can be viewed as the moving molecule creating strong fluctuations in the electron structure of the combined system.

In addition to conservative forces, there are dissipative forces. From the fluctuation-dissipation theorem point of view it is obvious that there are dissipative processes. As they appear beyond the adiabatic approximation they can also be characterized as non-adiabatic processes. From the previous sections it should be clear

that electron-structure changes are important for the potential-energy surfaces. The connection between fluctuations and dissipations implies that electronic transitions should be important as non-adiabatic effects. The parallel with the electron-phonon problem of solids [48] is apparent.

The role of the non-adiabatic processes is to introduce the element of irreversibility into the course of events. It is only through sufficiently strong dissipative forces and thus inelastic scattering that the molecule can loose enough kinetic energy to be trapped in the potential-energy well at the surface. It is only through non-adiabatic transitions that real transition or intermediate states are created.

Although the importance of non-adiabatic processes were stressed already at, e.g., the Gstaad meeting [48,49], the description of such processes is still in its infancy. We will here briefly review some recent developments that some of us have been involved in, with particular emphasis on the role of shifted and broadened affinity levels.

*Surface chemiluminescence.* A radiative transition occurs, when an electron jumps from a higher energy level to a lower one. In a many-electron system, this can occur by an initially highly excited electron falling down to a level above the Fermi level or by a Fermi sea electron falling into some hole in the electron distribution. In surface reactions, such excited electron or hole states can be created by filled ionization levels being pushed up in energy or by empty affinity levels being shifted downwards. The latter case will here be briefly illustrated by a MO description of surface chemiluminescence from halogen molecules hitting a sodium surface [50], which has recently been proposed by Newns and two of us [7].

For a molecule moving infinitely slowly, there would be ample time to adiabatically fill all levels that are pushed below the Fermi level, and there would be zero probability for a hole transition state. Rapidly moving molecules are required for the non-adiabatic processes, which are necessary to get such states. Actually, the adsorbate resonance width  $\Delta_a$  in eq. (7) here gets a real physical manifestation. With  $w(t)dt = (2\Delta_a/\hbar)dt$  being the probability that a hole in an adsorbate MO  $|a\rangle$  will decay between the times  $t$  and  $t + dt$ , the probability that the hole will persist until a time  $t$  is

$$P_h(t) = \prod_{t' < t} [1 - w(t') dt'] = \exp \left[ - \int_{-\infty}^t w(t') dt' \right]. \quad (14)$$

If, for simplicity, the velocity of the adsorbate towards the surface is assumed to be constant, the  $t$  dependence can be transformed into a dependence on the adsorbate position  $z = vt$ :

$$P_h(z) = \exp \left[ - \frac{2}{\hbar v} \int_{z_1}^z \Delta_a(z') dz' \right]. \quad (15)$$

The integration is here only from the point  $z_1$ , where the affinity level  $\epsilon_a(z)$  crosses the Fermi level.

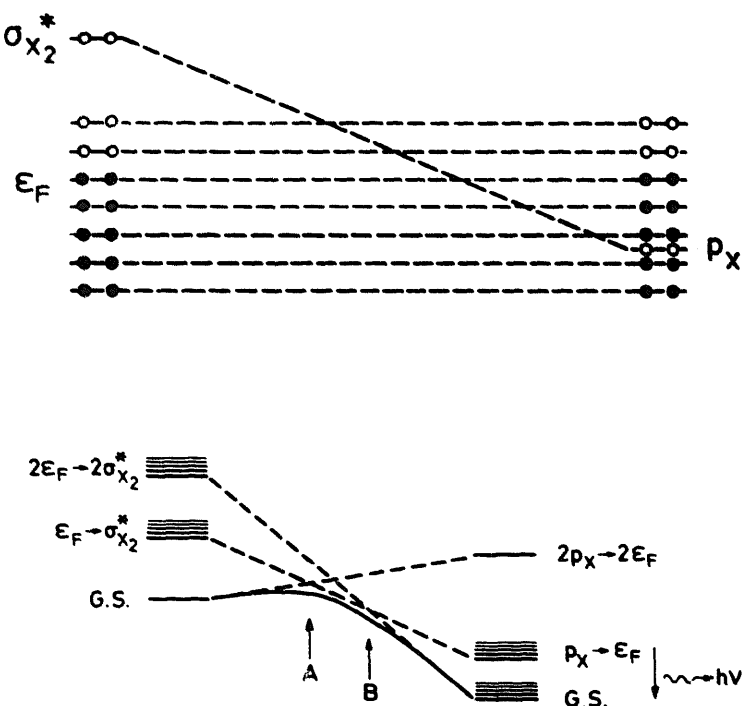


Fig. 18. Approximate orbital (a) and total state (b) correlation diagrams for halogen ( $X_2$ ) chemisorption on a metal with the Fermi energy  $\epsilon_F$  [7]. The label  $p_X$  stands for the p-type resonance, induced by a halogen atom X. The label  $p_X \rightarrow \epsilon_F$  means that one electron has moved from this resonance to a level close to the Fermi level.

The energy level  $\epsilon_a(z)$  and its variation with the distance  $z$  from the surface has been estimated from a model for the dissociative adsorption of halogen molecules on alkali metals, which has been inferred from the above-mentioned results for  $H_2$  on jellium and from the description of the corresponding gas-phase dimer-dimer reaction [51]. For a halogen molecule  $X_2$  getting adsorbed on, e.g., an Na surface, there are initially two unoccupied  $\sigma_{X_2}^*$  spin-orbitals, and at the completion of the process there are two adsorbed X atoms with filled p shells [23]. The schematic orbital and total-state correlation diagrams in fig. 18 indicate that in the adiabatic process the transfer of electrons occurs in two steps: an electron jump (harpooning) at the point A and an electron transfer at B. Non-adiabatic processes may occur, however, which leave a hole in the p resonance. Light emission can then occur by metal electrons filling this hole radiatively.

By using realistic estimates for  $\epsilon_a(z)$ ,  $\Delta_a(z)$ ,  $v$  and the radiative transition probability, results for  $P_h$  and the chemiluminescence spectra have been obtained [7]. It is noteworthy that the region, where the hole probability  $P_h(z)$  goes from 1 to 0, is rather narrow and lies well outside the adsorption equilibrium position. The comparison with the experimental spectra (fig. 19) for  $Cl_2$ ,  $Br_2$  and  $I_2$  on sodium [50] show that the theoretical curves are in the right energy range, that the trend for the

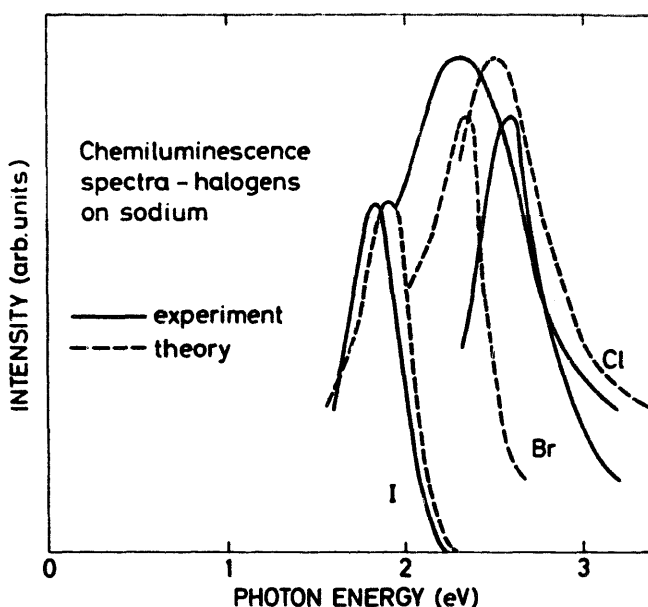


Fig. 19. Comparison of experimental [50] and theoretical chemiluminescence spectra from halogen adsorption on sodium [7].

high-energy cut-off through the halogen series is the right one, and that the curve shapes are reasonable, except for the too slow tailing-off on the low-energy side. The general agreement is taken as a support for the described picture of surface chemiluminescence.

The description has been extended to other chemiluminescent system, for instance O<sub>2</sub> on Al [8]. The experimental fact that at low coverage the broad maximum in the emission spectrum lies around an energy value (2.2 eV) much smaller than the 2p-electron binding energy of 6–7 eV measured by ultraviolet photoemission here gets an explanation in terms of the level variation  $\epsilon_a(z)$ , calculated by Lang and Williams [23], and the fact that the radiative filling of the hole should occur significantly outside the equilibrium position of adsorbed O.

In the above perspective, surface chemiluminescence appears as a most useful experiment. It definitely shows that an energy dissipation into photons is occurring, and it is an informative indicator of intermediate states in certain surface reactions. The information is complementary to that obtained by “ordinary” spectroscopies, as it measures the energy of the state at a distance from the surface, where important electron distributions are occurring, and not at the equilibrium position.

*Electron emission upon chemisorption.* The intermediate state can also decay through Auger transitions, either directly or after hopping into the substrate [8]. A cascade of electron-hole pairs is likely to occur. In a regular experimental situation the majority of these decay products are not observed, however. Only electrons excited above the work-function barrier can be detected. An increase in the yield of emitted electrons upon a decrease in the work function has been observed for some

systems [8]. This gives a qualitative support for the picture above.

**Sticking.** For an atom or molecule to stick to a surface, it is not sufficient with an attractive potential–energy surface. To be trapped in the surface potential well, the adsorbate has to both reach the well and, once there, loose sufficiently much of its kinetic energy to avoid being quasi-elastically scattered back from the surface. These two aspects are expressed by writing the thermally averaged initial sticking probability as

$$s_0 = \sigma \exp(-E_a/kT). \quad (16)$$

Here,  $E_a$  is the activation energy of a possible barrier outside the well, and  $\sigma$  is the so called condensation coefficient, which is related to the probability that the adsorbate looses a kinetic energy of the order  $kT$  in the well.

Various mechanisms for the energy dissipation have been proposed, including an electronic one [8]. Due to the non-zero velocity of the impinging adsorbate, the system is likely to end up in an excited electronic state, as described above. For the common case, where holes are introduced in the adsorbate-induced electron structure below the Fermi level, by initially empty adsorbate states being shifted down and broadened upon approaching the surface, many of the results in sections 2–4 can be utilized. A qualitative and quantitative analysis of this mechanism shows that the conditions for a large  $\sigma$  (close to unity) are (i) that the adsorbate electron structure has a resonance, which is (partially) filled or emptied during the adsorption process, and (ii) that the normal velocity of the adsorbate is high during the filling or emptying [8]. Condition (i) should be fulfilled for many atomic and molecular adsorbates on metal surfaces. An example of manipulation of the electronic structure to reduce  $\sigma$  is given by co-adsorption of K and CO on an Fe surface [52]. The velocity should vary from one adsorbate to another, from one substrate to another, and from one surface to another. The factor (ii) is therefore the most important one in explaining the specificity of  $\sigma$ .

**Ion emission.** A related phenomenon, where non-adiabatic processes at surfaces seem to be essential, is ion emission. This process is of importance for, e.g., secondary ion mass spectroscopy (SIMS) for chemical analysis and in the design of ion sources based on the sputtering technique. An essential quantity in the description of the sputtering process is the probability  $\alpha^{+(-)}(E)$  that the sputtered particle comes out of the material as a positive (negative) ion. Two of us have recently looked into the question, how  $\alpha^{+(-)}$  depends on the physical properties of the sputtered particle and the ejecting substrate, and on the kinetic energy of the ejected particle [53].

The experience of the shifting and broadening of adsorbate ionization and affinity levels  $\epsilon_a(z)$  in a narrow  $z$  region is of importance. To get the leading dependencies on parameters like the work function  $\phi$  and the atomic affinity  $A$  (or ionization potential  $I$ ), a simple interpolation formula has been used for  $\epsilon_a(z)$ . With reasonable parameters also for the resonance width and the outward velocity  $v$  of the secondary ion, the ionization probability for a large class of systems has been

shown to be roughly proportional to  $\exp\{-(I-\phi)/cv\}$  for positive ions and  $\exp\{-(\phi-A)/cv\}$  for negative ions,  $c$  being a constant [53]. This theoretical description reproduces experimental trends in the parameter dependencies. It is also internally consistent, as far as the orders of magnitudes of the model constants are concerned.

## 5. Concluding remarks

This paper has reviewed some theoretical studies of the molecule–metal interaction and of surface reactions that we have recently been involved in. An attempt has been made to summarize some of the results in a simple, and probably slightly over-simplified thesis: *The high reactivity of metals is due to the high polarizability of the metal conduction electrons.*

By the high reactivity of metals one usually means their good ability to break chemical bonds and to otherwise catalyze chemical reactions. To illustrate the former, we have in section 3 reviewed results for H<sub>2</sub> adsorption from self-consistent model calculations and applied a simple conceptual model to explain trends in the adsorption of CO. To illustrate the latter, disproportionation of CO on Ni surfaces has also been described in section 3. The ability to get molecules and atoms to stick to the surface is also important for the reactivity of metals. In section 4 we have described an electronic dissipation mechanism for the sticking. It involves the creation of an intermediate hole state, whose existence has been verified in some surface chemiluminescence experiments, and which seems to be consistent with measured emission of electrons in some exothermic reactions. In all these illustrations, the pulling down and broadening of adsorbate affinity levels and their adiabatic or non-adiabatic filling have been key features, whose detailed nature has been extracted from self-consistent model calculations.

Section 2 about adsorbate-induced electron structure is aimed at a better understanding of these level shifts and fillings. Self-consistent model calculations show the importance of metal substrate parameters, in particular the intrinsic correlation with the effective electron potential of the clean surface. The consequent multiple filling of the affinity-levels carries an energy cost, which is significantly smaller than in a free atom or molecule. The reasons why the intraatomic or -molecular Coulomb repulsion is circumvented are clearly illustrated in the limiting model case of a hydrogen atom in jellium, where orbital and screening charges can be separated. A Coulomb hole is created around the pseudo-ion (H<sup>-</sup>), and the interpenetration of orbital and screening charges reduces the effective Coulomb repulsion between the electrons occupying the orbital. These two metallic screening effects are due to the high polarizability of the conduction electrons.

The firm establishment of simple rules like the above thesis obviously requires more self-consistent calculations on other systems and more analyzes of other surface reactions. This should be a very interesting challenge.

## Acknowledgements

During the course of the work reviewed here the authors have benefitted from stimulating discussions with many people, including D. Adams, S. Andersson, B. Kasemo, S. Lundqvist, J.P. Muscat, D.M. Newns, K. Schönhammer and B. Vinter. This project has been partially supported by the Swedish Natural Science Research Council.

## References

- [1] Physical Basis for Heterogeneous Catalysis, Eds. E. Drauglis and R.L. Jaffee (1975); see, in particular, the discussion on p. 476.
- [2] O. Gunnarsson, H. Hjelmberg and B.I. Lundqvist, Phys. Rev. Letters 37 (1976) 292; Surface Sci. 63 (1977) 348.
- [3] H. Hjelmberg, O. Gunnarsson and B.I. Lundqvist, Surface Sci. 68 (1977) 158.
- [4] (a) H. Hjelmberg, Phys. Scripta 18 (1978) 481;  
 (b) H. Hjelmberg, Surface Sci. 81 (1979) 539.
- [5] B.I. Lundqvist, J.K. Nørskov and H. Hjelmberg, Surface Sci. 80 (1979) 441;  
 J.K. Nørskov, H. Hjelmberg and B.I. Lundqvist, Solid State Commun. 28 (1978) 899.
- [6] H. Hjelmberg, B.I. Lundqvist and J.K. Nørskov, Phys. Scripta, in print.
- [7] J.K. Nørskov, D.M. Newns and B.I. Lundqvist, Surface Sci. 80 (1979) 179.
- [8] B. Kasemo, E. Törnqvist, J.K. Nørskov and B.I. Lundqvist, Surface Sci. 89 (1979) 554.
- [9] J.K. Nørskov and B.I. Lundqvist, Surface Sci. 89 (1979) 251.
- [10] S. Andersson, B.I. Lundqvist and J.K. Nørskov, in: Proc. 7th Intern. Vacuum Congr. and 3rd Intern. Conf. on Solid Surfaces, Vienna, 1977, p. 815.
- [11] O. Gunnarsson, H. Hjelmberg and J.K. Nørskov, to be published.
- [12] W. Kohn and L.J. Sham, Phys. Rev. 140 (1965) A1133.
- [13] See, e.g., O. Gunnarsson and B.I. Lundqvist, Phys. Rev. B13 (1976) 4274.
- [14] O. Gunnarsson, in: NATO, Advanced Study Institute Series, Vol. 42, Electrons in disordered metals and at metallic surfaces, Eds. P. Phariseau and B.L. Gyorffy.
- [15] See, e.g., B. Vinter, Phys. Rev. B17 (1977) 2429.
- [16] See, e.g., N.D. Lang, Solid State Phys., 28 (1973) 225.
- [17] The spirit of this approach is given in, e.g., the textbook by N.W. Ashcroft and N.D. Mermin, Solid State Physics (Holt, Rinehart and Winston, New York, 1976).
- [18] C.O. Almlöd, U. von Barth, Z.D. Popovic and M.J. Stott, Phys. Rev. B14 (1976) 2250.
- [19] J.K. Nørskov, Solid State Commun. 24 (1977) 691; Solid State Commun. 25 (1978) 995; Phys. Rev. B, in print.
- [20] The singly occupied level is found to be 0.059, 0.19, 0.29 and 0.32 Ryd below the bottom of the conduction band for  $r_s = 2.07, 2.65, 3.93$  and 6, respectively, according to the calculations in ref. [19].
- [21] R.W. Gurney, Phys. Rev. 47 (1935) 479.
- [22] D.M. Newns, Phys. Rev. 178 (1969) 1123.
- [23] N.D. Lang and A.R. Williams, Phys. Rev. Letters 37 (1976) 212; Phys. Rev. B18 (1978) 616.
- [24] For recent reviews about the adsorbate-induced electron structure, see, e.g.,  
 B.I. Lundqvist, H. Hjelmberg and O. Gunnarsson, in: Photoemission and the Electronic Properties of Surfaces, Eds. B. Feuerbacher, B. Fitton and R.F. Willis (Wiley, New York, 1978);  
 J.P. Muscat and D.M. Newns, Progr. Surface Sci. 9 (1978) 1.

- [25] The affinity value of H in the local-density approximation has been taken from O. Gunnarsson, B.I. Lundqvist and J.W. Wilkins, Phys. Rev. B10 (1974) 1319.
- [26] T.F. O'Malley, in: Advances in Atomic and Molecular Physics, Vol. 7, Eds. D.R. Bates and I. Easterman (Academic Press, New York, 1971) p. 223.
- [27] As summarized in, e.g., J.W. Gadzuk, Surface Sci. 43 (1979) 44.
- [28] K.H. Johnson, Intern. J. Quantum Chem. S11 (1977) 39.
- [29] See, e.g., J. Harris and G.S. Painter, Phys. Rev. Letters 36 (1976) 151.
- [30] D.E. Ellis and G.S. Painter, Phys. Rev. B2 (1970) 2887;  
E.J. Baerends and P. Ros, Mol. Phys. 30 (1975) 1735, and private communication.
- [31] Louie, Phys. Rev. Letters 42 (1979) 476.
- [32] A.B. Anderson and R. Hoffmann, J. Chem. Phys. 61 (1974) 4545.
- [33] J.E. Lennard-Jones, Trans. Faraday Soc. 28 (1932) 333.
- [34] K. Ruedenberg, Rev. Mod. Phys. 34 (1962) 326.
- [35] C. Kittel, Introduction to Solid State Physics, 3rd ed. (Wiley, New York, 1966) p. 79.
- [36] Thermodynamically, the separation into such clear-cut cases cannot be made, until lattice corrections have been introduced, as in fig. 15. Then it might be the case that the associatively adsorbed H<sub>2</sub> on Na is only a precursor state. These aspects should not be important for the qualitative considerations here, however.
- [37] See, e.g., G. Brodén, T.N. Rhodin, C. Brucker, R. Bentzon and Z. Haryck, in: Photoemission from Surfaces, extended abstracts of papers presented at Noordwijk Meeting, September 1976, ESA-SP118 preprint, p. 177;  
T.N. Rhodin and C.F. Brucker, Solid State Commun. 23 (1977) 275.
- [38] See, e.g., G. Doyen and G. Ertl, Surface Sci. 43 (1974) 197.
- [39] The importance of the role of d electrons in the adsorption of H<sub>2</sub> has been emphasized by D.M. Newns [22,24]. For a more complete discussion of the effects of the d-electrons on the activation energy for H<sub>2</sub> dissociation, see D.M. Newns, J.K. Nørskov and B.I. Lundqvist, to be published.
- [40] The parameters used in eq. (10) have been taken from D.J.M. Fassaert and A. van der Avoird, Surface Sci. 55 (1976) 291.
- [41] The authors are grateful to J. Lindberg for providing the calculated overlap integrals and energy parameters.
- [42] M. Balooch and R.E. Stickney, Surface Sci. 44 (1974) 310;  
M. Balooch, M.J. Cardillo, D.R. Miller and R.E. Stickney, Surface Sci. 46 (1974) 358.
- [43] E.J. Baerends and P. Ros, Mol. Phys. 30 (1975) 1735;  
See also ref. [6] for H<sub>2</sub>.
- [44] See, e.g., I.P. Batra and P.S. Bagus, Solid State Commun. 16 (1975) 1097.
- [45] R.G. Pearson, Acc. Chem. Rev. 4 (1979) 152.
- [46] R. Hoffmann and R.B. Woodward, in: The Conservation of Orbital Symmetry (Academic Press, New York, 1970).
- [47] E.K. Rideal, Concepts in Catalysis (Academic Press, New York, 1968).
- [48] J.R. Schrieffer, in: ref. [1], p. 576.
- [49] M. Boudart, T.B. Grimley and D.M. Newns, in: ref. [1], p. 576.
- [50] B. Kasemo and L. Walldén, Surface Sci. 53 (1975) 393.
- [51] See, e.g., W.S. Struve, I.R. Krenos, D.L. McFadden and D.R. Herschbach, J. Chem. Phys. 62 (1975) 404.
- [52] G. Brodén, G. Gafner and H.P. Bonzel, Surface Sci. 84 (1979) 295.
- [53] J.K. Nørskov and B.I. Lundqvist, Phys. Rev. B19 (1979) 5661.